[3]F. Kerger *et al.*, in *Plasma Physics and Controlled Nuclear Fusion Research* (International Atomic Energy Agency, Vienna, 1975).
[4]S. von Goeler *et al.*, Phys. Rev. Lett. 33, 1201 (1971).
[5]V. D. Shafranov, Sov. Phys. Tech. Phys. 15, 175 (1970).
[6]S. Inoue, K. Itoh, and S. Yoshikawa, Institute for Plasma Physics of Japan Report No. 212, 1974 (unpublished), and Phys. Lett. 53A, 342 (1975).
[7]H. P. Furth *et al.*, Phys. Fluids 16, 1054 (1973).
[8]H. P. Furth *et al.*, Phys. Fluids 6, 459 (1963).
[9]K. Makishima *et al.*, to be published.
[10]T. Tominaga *et al.*, to be published.
[11]V. D. Shafranov and E. I. Yurchenko, Zh. Eksp. Teor. Fiz. 53, 1157 (1967) [Sov. Phys. JETP 26, 682 (1968)].
[12]M. N. Rosenbluth *et al.*, Phys. Fluids 16, 1894 (1973).

Observation of Two-Dimensional Plasmons and Electron-Ripplon Scattering in a Sheet of Electrons on Liquid Helium

C. C. Grimes and Gregory Adams
Bell Laboratories, Murray Hill, New Jersey 07974
(Received 12 November 1975)

The two-dimensional plasmon dispersion relation $\omega_p^2 = 2\pi Ne^2k/m$ has been verified in the classical one-component plasma formed by a sheet of electrons in image-potential–induced surface states on liquid helium. For temperatures below 0.68 K the plasmon damping indicates that the electron mobility is limited by electron-ripplon scattering.

We report an experimental study of plasmon propagation and damping in the two-dimensional (2D) classical plasma formed by a sheet of electrons in image-potential–induced surface states outside liquid helium. To our knowledge, this is the first time its peculiar dispersion relation has been verified. Furthermore, from the plasmon damping, we deduce the electron mobility and find—for the first time—strong evidence that at low temperatures the electrons are predominantly scattered by capillary waves (ripplons).

The prediction by Cole and Cohen[1] and by Shikin[2] that electrons can be bound in surface states outside certain bulk dielectrics such as He and Ne stimulated experimental searches for such states. Although the evidence for bound states in some early experiments[3,4] was questioned,[5] cyclotron resonance[6] showed that the electron motion on liquid helium is 2D and the electrons have the free-electron mass, while millimeter-wave spectroscopy[7] has firmly established that electrons are bound to a helium surface with an energy of 8 K. Consequently, at 1 K and below the electrons are predominantly in the ground state within the image-potential well and are localized within ≈ 100 Å of the helium surface, but they remain free to move parallel to the surface. Sommer and Tanner[3] found that from 0.9 to 2.0 K the electron mobility μ was limited by scattering from atoms in the He vapor, and μ had reached 2×10^6 cm^2/V sec at 0.9 K. In these experiments the surface-state electrons behaved like a highly mobile, classical, one-component, 2D plasma of variable density.

The 2D plasmon dispersion relation was first derived by Ritchie[8] and by Ferrell[9] who were treating characteristic energy loss of electrons in metal foils. Subsequently Stern[10] and Chaplik[11] have discussed plasmons in the 2D Fermi gas found in metal-oxide-semiconductor devices while Fetter[12] and Platzman and Tzoar[13] have considered the classical 2D electron gas which is of interest to us. The dispersion relation applicable to our experiment is obtained in the small-k limit ($kv/\omega_p \ll 1$) and with small damping ($\omega_p\tau \gg 1$): $\omega_p^2 = 2\pi Ne^2km_0^{-1}(1+i/\omega_p\tau)$, where v is the electron thermal velocity and τ is a phenomenological relaxation time.

We study the plasmon dispersion and damping by exciting standing-wave resonances in the surface-state electron plasma contained within a rectangle parallelepiped cell approximately $1.9\times1.2\times0.18$ cm^3 in size. The cell is assembled from metal plates electrically isolated from one another so that potentials can be applied to them. The bottom plate consists of three sections, with the center section forming a 50-Ω strip line. The strip line is connected at one end through a coaxial line to a broad-band swept-frequency spectrometer[14] and has the other end terminated in a matched load.

The experimental procedure consists of condensing enough helium in the apparatus to partially fill the cell with liquid, applying appropri-

ate potentials to the plates, and then depositing electrons on the liquid surface by briefly heating a filament mounted in a small hole in the top plate. With the bottom (submerged) electrodes biased at a positive potential of a few volts relative to the other electrodes, electrons can be held for hours. In addition to a dc potential we apply a small (~0.1 V) audio-frequency potential (~5 kHz) to the top, sides, and ends of the cell. This potential serves to modulate the areal density of the 2D electron gas by modulating the area within which the electrons are confined. We then employ a conventional phase-sensitive detector at the modulation frequency as a second detector following the rf detector. The resulting signal is dA/dN, the derivative of the rf absorption with respect to electron density. This signal is displayed versus frequency on an x-y recorder.

A representative trace is shown in Fig. 1. The first three standing-wave resonances corresponding to 1, 3, and 5 nodes contained within the width of the cell are prominent in the trace. By reducing the holding voltage in increments, one can obtain a series of traces at differing N's from which the relation between standing-wave frequency and N can be extracted. Figure 2 presents a log-log plot of resonance frequencies versus charging potential V_0 for the most prominent modes.[15] The solid lines, whose significance is explained below, have a slope of 0.5. It is apparent that the frequency of each mode is proportional to $N^{1/2}$ as expected.

To calculate the expected plasmon standing-wave frequencies, the "infinite medium" dispersion relation must be corrected for the finite height of the cell. Physically, the images in the top and bottom electrodes of a long-wavelength plasmon tend to screen the Coulomb restoring force and lower the plasmon frequency. Also, allowing for simultaneous propagation of plasmons along the length L of the cell[16] as well as across the width W of the cell we obtain (omitting damping) the relation $\omega_p^2 = 2\pi Ne^2 m_0^{-1} \times [k_x^2 F(k_x) + k_y^2 F(k_y)]^{1/2}$, where $F(k_i) = 2\sinh k_i d \times \sinh k_i(h-d)/\sinh k_i h$. Here d is the helium depth, h is the cell height, $k_x = m\pi/W$, $k_y = n\pi/L$, and m and n are integers. The resonance modes are now identified by the two integers (m,n) very much like wave-guide modes. The calculated resonance frequencies with $n=2$, m an odd integer, and $d/h = 0.375$ are shown as solid lines in Fig. 2.[17] For $m \geq 5$ the geometrical correction terms $F(k_i)$ are nearly unity and the plasmon frequency varies as $k^{1/2}$. This is the expected signature of the 2D plasmon. It is a direct consequence of the fact that wavelike charge-density perturbations in 2D interact like lines of charge (λ^{-1} force law) while in 3D the interaction is between sheets of charge and the force is indepen-

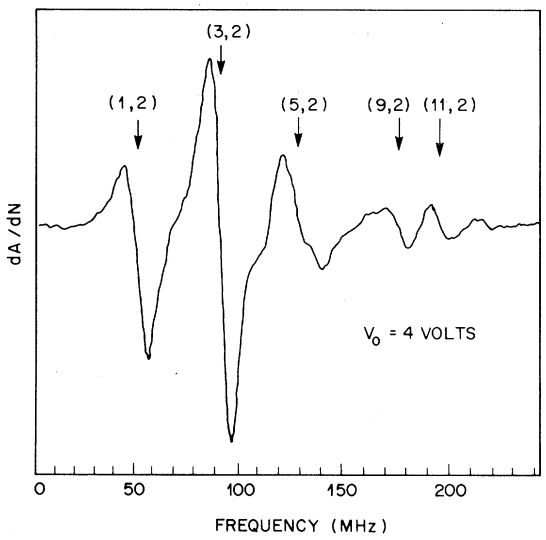

FIG. 1. Experimental trace of the derivative with respect to electron density of rf absorption plotted versus frequency. The resonances are due to plasmon standing-wave resonances whose calculated frequencies are indicated by arrows.

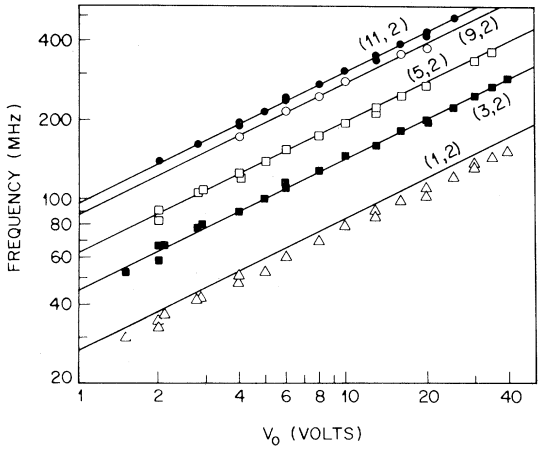

FIG. 2. Comparison of calculated and observed standing-wave resonance frequencies versus charging potential V_0. The surface charge density is $N = (8.6\times10^6)V_0$, where N is in electrons/cm^2 if V_0 is in volts. The agreement in slope and position in this plot verifies both the density and wave-vector dependence of the two-dimensional plasmon dispersion relation.

dent of λ.

From the linewidths of the standing-wave resonances we can deduce a phenomenological scattering time which is directly proportional to the electron mobility, μ, parallel to the helium surface. The electron mobility is expected to be governed by two scattering mechanisms: electron scattering by atoms in the helium vapor and scattering by ripplons on the liquid-helium surface. Gas-atom scattering is characterized by an approximately exponential decrease of μ with increasing temperature reflecting the increase in gas-atom density. At sufficiently low temperature the gas-atom scattering becomes negligible and electron-ripplon scattering governs μ. Electron-ripplon scattering is expected to be characterized by three phenomena: μ becomes temperature independent[1,2]; μ decreases as the electric field, $E_\perp$, pressing the electrons against the surface increases[2] (the perpendicular force enhances the electron-ripplon interaction); and μ becomes an increasing function of the electric field parallel to the surface for fields above a threshold value.[2,18] We have observed all three of these phenomena for $T < 0.68$ K.

The mobility is $\mu = e\tau/m_0$ with (assuming a Lorentzian line shape) $\tau = (2\pi 3^{1/2}\Gamma_{pp})^{-1}$, where Γ_{pp} is the linewidth measured between derivative extrema. In Fig. 3 we have plotted μ deduced from linewidths versus both T and the density of vapor atoms. Note that for T in the interval 0.48 to 0.68 K the vapor density changes by a factor of 100 while μ remains constant as predicted for ripplon scattering. The low-temperature limiting μ of $\approx 1.3\times 10^7$ cm^2/V sec with $E_\perp = 30$ V/cm is nearly two orders of magnitude larger than the ripplon-dominated μ calculated by Cole.[1] Above 0.68 K, μ decreases with increasing T, indicating that gas-atom scattering is becoming dominant.

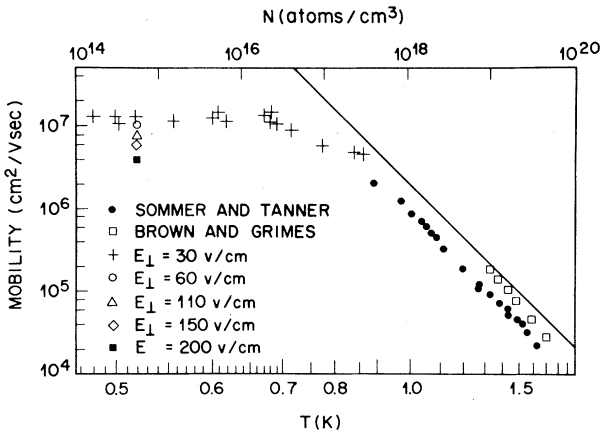

FIG. 3. Electron mobility versus temperature and helium-vapor density. Below 0.68 K the mobility is limited by ripplon scattering while at higher temperatures vapor-atom scattering predominates. The line from Brown and Grimes (Ref. 6) is a calculation for vapor-atom scattering only. The Sommer and Tanner data points are from Ref. 3.

For temperatures where ripplon scattering is significant, μ decreases rapidly with increasing $E_\perp$ as shown by the data points at 0.52 K. Our preliminary data at 0.52 K can be fitted by $\mu(E_\perp) = C(E_0 + E_\perp)^{-2}$ within the experimental error of $\pm 5\%$ using $C = 9.3\times 10^{11}$ V/sec and $E_0 = 230$ V/cm. This form for $\mu(E_\perp)$ reduces at large $E_\perp$ to that derived by Shikin[2] whose calculated value of C is about twice the observed value.

In the region where ripplon scattering predominates, dramatic nonlinear effects appear when the component of the rf field parallel to the helium surface exceeds a threshold of a few tens of millivolts per centimeter. The observed nonlinear increase in signal amplitude above threshold clearly indicates that μ is an increasing function of the rf electric field, thus confirming the non-Ohmic behavior anticipated by Crandall[18] and Shikin.[2]

In conclusion, we feel that the observed dependences of the electron mobility on temperature, of the plasmon standing-wave resonance linewidth on $E_\perp$, and of the resonance amplitude on rf drive level provide compelling evidence that electron-ripplon scattering predominates for $T \lesssim 0.68$ K. We hope that these measurements will provide a stimulus for others to refine the calculations of the ripplon-limited electron mobility in the weak external field regime.

We wish to thank R. S. Crandall, A. L. Fetter, J. J. Hauser, P. M. Platzman, C. L. Zipfel, G. G. Zipfel, and N. Tzoar for stimulating discussions. We are grateful to T. R. Brown for a continuing dialogue on all aspects of this work, and we are indebted to C. M. Antosh for evaporated metal film coatings on parts of the cell.

[1]Milton W. Cole and Morrel H. Cohen, Phys. Rev. Lett. 23, 1238 (1969); Milton W. Cole, Phys. Rev. B 2, 4239 (1970), and Rev. Mod. Phys. 46, 451 (1974).

[2]V. B. Shikin, Zh. Eksp. Teor. Fiz. 58, 1748 (1970), and 60, 713 (1971) [Sov. Phys. JETP 31, 936 (1970), and 33, 387 (1971)]; V. B. Shikin and Yu. P. Monarkha, J. Low Temp. Phys. 16, 193 (1974).

[3]W. T. Sommer and David J. Tanner, Phys. Rev. Lett. 27, 1345 (1971).

[4]R. Williams, R. S. Crandall, and A. H. Willis, Phys. Rev. Lett. 26, 7 (1971).
[5]R. M. Ostermeier and K. W. Schwarz, Phys. Rev. Lett. 29, 25 (1972).
[6]T. R. Brown and C. C. Grimes, Phys. Rev. Lett. 29, 1233 (1972).
[7]C. C. Grimes and T. R. Brown, Phys. Rev. Lett. 32, 280 (1974); C. C. Grimes, T. R. Brown, Michael L. Burns, and C. L. Zipfel, to be published.
[8]R. H. Ritchie, Phys. Rev. 106, 874 (1957).
[9]Richard A. Ferrell, Phys. Rev. 111, 1214 (1958).
[10]Frank Stern, Phys. Rev. Lett. 18, 546 (1967).
[11]A. V. Chaplik, Zh. Eksp. Teor. Fiz. 62, 746 (1972) [Sov. Phys. JETP 35, 395 (1972)].
[12]Alexander L. Fetter, Ann. Phys. (N.Y.) 81, 367 (1973), and Phys. Rev. B 10, 3739 (1974).
[13]P. M. Platzman and N. Tzoar, to be published.
[14]The spectrometer is based on a coaxial hybrid junction. See Melvin P. Klein and Donald E. Phelps, Rev. Sci. Instrum. 38, 1545 (1967).
[15]The electron density is calculated using the known dimensions of the cell, the applied potentials, and the helium depth which is roughly determined in a capacitance measurement.
[16]If the cell is not perfectly level, plasmon modes having a full wavelength variation along the length of the cell can be excited.
[17]We must take m equal to an odd integer so that the modes have the same symmetry as the driving rf field, and we take $n=2$ corresponding to a full wavelength in L. The mode with $m=7$ is only very weakly excited because the corresponding spatial Fourier component of the driving rf field is small.
[18]R. S. Crandall, Phys. Rev. A 6, 790 (1972).

Electron-Energy-Loss Spectroscopy of Semiconducting SmS(100): Evidence for a Surface Phase Transition

J. E. Rowe, M. Campagna, and S. B. Christman
Bell Laboratories, Murray Hill, New Jersey 07974

and

E. Bucher
Universität Konstanz, D-775, Konstanz, Germany

(Received 23 September 1975)

The presence of trivalent Sm has been observed near the (100) surface of pure semiconducting SmS using electron-energy-loss spectroscopy with 100-eV electrons. This surface phase transition is interpreted as due to differential contraction of the surface cation lattice constant for NaCl-type (100) surfaces and helps to resolve reported differences in ultraviolet and x-ray photoemission experiments on SmS.

The nature of the wave function of Sm in both the semiconducting ("black") and the high-pressure ("golden") metallic phase has recently generated considerable interest. Above the semiconductor-metal phase transition at 6.5 kbar, or in "golden" substituted alloys with a variety of cations and anions, Sm in SmS is by now accepted to be in an intermediate-valence or interconfiguration-fluctuation (ICF) state[1] with a time-average nonintegral number of $4f$ electrons (5.3). In contrast, different conclusions have been reached for semiconducting SmS. Upper limits of ~10% and ~3% for the valence mixing in the black phase have been obtained from inelastic neutron scattering[2] and x-ray photoemission spectroscopy (XPS),[1] respectively. Evidence for a larger configurational mixing of at least 15% has been reported using ultraviolet photoemission spectroscopy (UPS) with synchrotron radiation.[3] All of these experiments have been interpreted with the assumption that the bulk electronic structure of rare-earth compounds persists into the surface region. We show below that this is not true for SmS(100) and that a surface mixed-valence phase occurs even for undoped semiconducting SmS as a result of surface lattice-constant relaxation which decreases the Sm-Sm distance normal to the surface by ~0.2–0.4 Å.

We report in this Letter results of the first electron-energy-loss spectroscopy (ELS) of pure, "black" SmS (100) cleavage surfaces. The data strongly suggest that the clean, equilibrium surface layer of semiconducting SmS contains Sm ions with both valences, unlike the bulk phase of SmS. Whether this coexistence of divalent and trivalent Sm is related to a two-dimensional ICF state is at present unclear. The mixed-valence